Available online at www.sciencedirect.com

ScienceDirect

Journal of Ocean Engineering and Science 1 (2016) 149–156

www.elsevier.com/locate/joes

Reliability evaluation of the roll motion under the wind and irregular beam waves

Wei Chai*

Department of Marine Technology, Norwegian University of Science and Technology, Trondheim, Norway

Received 14 August 2015; received in revised form 18 November 2015; accepted 17 December 2015
Available online 16 March 2016

Abstract

This paper intends to study the stochastic response and reliability of the roll motion under the action of wind and wave excitation. The roll motion in random beam seas is described by a four-dimensional (4D) Markov dynamic system whose probabilistic properties are governed by the Fokker–Planck (FP) equation. The 4D path integration (PI) method, an efficient numerical technique based on the Markov property of the 4D system, is applied in order to solve the high dimensional FP equation and then the stochastic statistics of the roll motion are derived. Based on the obtained response statistics, the reliability evaluation of the ship stability is performed and the effect of wind action is studied. The accuracy of the 4D PI method and the reliability evaluation is assessed by the versatile Monte Carlo simulation (MCS) method.

Keywords: Path integration method; Stochastic roll response; Reliability evaluation; Wind action; Monte Carlo simulation.

1. Introduction

The roll motion in random seas is the most critical mode leading to ship stability failure. Generally, there are two types of intact stability failures, i.e., total intact stability failure and partial stability failure [1]. Ship capsizing is classified as the former category, while the latter is associated with the occurrence of large or extreme roll angles, which would impair the normal operations or even lead to damage of the ship. Therefore, prediction of the extreme roll responses and the associated risk assessment of ship stability are crucial for reliability based design and operation in practice.

However, the current criteria of the International Maritime Organization (IMO) for evaluation of the intact stability of a vessel under the action of random wave and wind excitation are simply based on the weather criterion. This criterion is hydrostatic and the stochastic properties of the external excitation have not been taken into consideration. In this study, the dynamic stability is evaluated by means of a probabilistic approach and the associated stochastic roll response as well as the reliability evaluation may provide insight with respect to the effect of random external excitation on the nonlinear roll dynamics.

The mean upcrossing rate is a key parameter for a detailed assessment of the response statistics of marine structures subjected to random excitation loads [2]. Moreover, the reliability analysis methodology based on the mean upcrossing rate is robust and widely used in the reliability engineering. However, determining the stochastic response (such as the mean upcrossing rate) of the nonlinear roll motion excited by random external excitation is a challenge and limited progress has been made in the past decades. Monte Carlo simulation (MCS) is the simplest methodology to determine the mean upcrossing rate of the roll motion, but the associated computation burden may be prohibitive for estimation of the high-level responses with low probability levels.

In addition to the versatile and straightforward MCS method, the methodology based on the Markov diffusion theory is attractive since the probabilistic properties are governed by the Fokker–Planck (FP) equation [3]. It is well known that the Markov model is only valid for the dynamic systems driven by Gaussian white noise or filtered white noise. Therefore, the shaping filter technique is introduced in order

* Corresponding author.
E-mail address: chai.wei@ntnu.no.

http://dx.doi.org/10.1016/j.joes.2016.03.003

to approximate the random external excitation term as a filtered white noise process. For the extended Markov system, established by combining the roll motion equation and the filter model, the efficient path integration (PI) method is applied in order to obtain the response statistics by solving the corresponding FP equation. The main advantage of the PI method and the Markov dynamic system is that a host of accurate and useful response statistics can be obtained within one calculation [4,5]. Moreover, the great performance and high efficiency of the PI technique in calculating the mean upcrossing rate of high-level roll responses will be demonstrated.

In this paper, we aim to quantify the wind action on the stochastic roll response as well as on the intact ship stability. The MCS method serves as an efficient tool to evaluate the accuracy of the proposed numerical methods. The results and conclusions obtained in this work hopefully can provide useful references for ship stability research and practical operations.

2. Mathematical model of roll motion

For the case of dead ship condition, i.e. a ship with zero speed (or low speed) under unidirectional beam seas and beam wind action, the roll motion can be represented by the following single-degree-of-freedom (SDOF) equation [6]:

$$(I_{44}+A_{44})\ddot{\theta}(t)+B_{44}\dot{\theta}(t)+B_{44q}\dot{\theta}(t)|\dot{\theta}(t)| + \Delta GZ(\theta(t))=M_{wave}(t)+M_{wind}(t) \tag{1}$$

where $\theta(t)$ and $\dot{\theta}(t)$ are the roll angle and the roll velocity, respectively. I_{44} represents the moment of inertia in roll and A_{44} is the added mass moment term. B_{44} and B_{44q} are linear and quadratic damping coefficients, respectively. The stiffness term $\Delta GZ(\theta(t))$ relates to the restoring moment of the roll motion, $M_{wave}(t)$ represents the random wave excitation moment and $M_{wind}(t)$ denotes the excitation moment caused by wind.

The restoring moment is expressed in terms of the displacement Δ and the restoring arm GZ, which can be obtained from standard hydrostatic software. The restoring moment term is usually given by a nonlinear odd function of the roll angle, i.e.

$$GZ(\theta)=C_1\theta-C_3\theta^3 \tag{2}$$

in which, C_1 and C_3 are the linear and the nonlinear roll restoring coefficients of the restoring arm, respectively. Note that the roll motion has a softening characteristic since the nonlinear stiffness term is negative. For the softening cases, ship capsizing would happen when the roll angle exceeds the angle of vanishing stability beyond which the restoring moment becomes negative.

The random wave excitation moment $M_{wave}(t)$ can be described by the wave excitation moment spectrum, $S_{Mwave}(\omega)$. The latter is related to the wave energy spectrum, $S_{\xi\xi}(\omega)$, by the following relationship:

$$S_{M_{wave}}(\omega)=|F_{roll}(\omega)|^2 S_{\xi\xi}(\omega) \tag{3}$$

where $|F_{roll}(\omega)|$ represents the roll moment amplitude per unit wave height at frequency ω. Moreover, the wave elevation and the wave excitation moment are assumed to be stationary Gaussian processes.

For the wind induced excitation moment, $M_{wind}(t)$, it can be calculated by the following formula:

$$M_{wind}(t)=\frac{1}{2}\rho_{air}C_wA_wl_W(U_m+U(t))^2 \tag{4}$$

where ρ_{air} is the mass density of air and C_w denotes a wind pressure coefficient. U_m is the mean wind speed and $U(t)$ is the fluctuating wind speed. A_w represents the lateral windage and l_w is the wind moment arm.

Generally, $(U(t)/\ U_m)<<1$ and the wind excitation moment (4) can be expressed as [7]:

$$\begin{aligned}M_{wind}(t)&=\bar{M}_{wind}+M_f(t)\\&=\frac{1}{2}\rho_{air}C_wA_wl_WU_m^2+\rho_{air}C_wA_wl_WU_mU(t)\end{aligned} \tag{5}$$

where $\bar{M}_{wind}$ and $M_f(t)$ denote the mean wind moment and fluctuating wind moment, respectively. The mean wind action results in a heeling angle θ_s and their relationship can be expressed as:

$$\bar{M}_{wind}=\Delta GZ(\theta_s) \tag{6}$$

As for the fluctuating wind moment, its spectral density is related to the wind spectrum $S_U(\omega)$, by the following relationship [2]:

$$S_{M_f}(\omega)=(\rho_{air}C_wA_wl_WU_m)^2\cdot\chi(\omega)\cdot S_U(\omega) \tag{7}$$

where $\chi(\omega)$ is the aerodynamic admittance function, which can be determined as:

$$\chi(\omega)=\frac{1}{1+(\frac{\omega\sqrt{A_w}}{\pi U_m})^{4/3}} \tag{8}$$

The wind spectrum, which governs the fluctuating wind speed, is given by the Davenport spectrum:

$$S_U(\omega)=4K\frac{U_m^2}{\omega}\frac{X_D^2}{(1+X_D^2)^{4/3}} \tag{9}$$

where $K=0.003$ and the dimensionless variable X_D is given by the following equation [8]:

$$X_D=600\frac{\omega}{\pi U_m} \tag{10}$$

Dividing Eq. (1) by $(I_{44}+A_{44})$, the final format of the differential equation is given as:

$$\begin{aligned}&\ddot{\theta}(t)+b_{44}\dot{\theta}(t)+b_{44q}\dot{\theta}(t)|\dot{\theta}(t)|+c_1\theta(t)-c_3\theta^3(t)\\&=(m_{wave}(t)+m_f(t))+\bar{m}_{wind}=m(t)+\bar{m}_{wind}\end{aligned} \tag{11}$$

where b_{44}, b_{44q}, c_1, c_3 are relative ship parameters. $m_{wave}(t)$, $m_f(t)$ and $\bar{m}_{wind}$ are relative moments. The total relative random external excitation is denoted as $m(t)$, which is assumed to be the sum of the relative wave excitation $m_{wave}(t)$ and the relative fluctuating wind moment $m_f(t)$. Correspondingly, the spectrum of $m(t)$ can be given as the sum of the spectrum of

the relative wave excitation moment and the spectrum of the relative fluctuating wind moment:

$$S_m(\omega) = (S_{M_{wave}}(\omega) + S_{M_f}(\omega))/(I_{44} + A_{44})^2 = S_{m_{wave}}(\omega) + S_{m_f}(\omega) \tag{12}$$

Finally, the SDOF model, i.e. Eq. (11), can be transformed into the state-space equation written as:

$$\begin{cases} dx_1 = x_2 dt \\ dx_2 = (-b_{44}x_2 - b_{44q}x_2|x_2| - c_1x_1 + c_3x_1^3 + x_3 + \bar{m}_{wind})dt \end{cases} \tag{13}$$

where $x_1 = \theta(t)$, $x_2 = \dot{\theta}(t)$, $x_3 = m(t)$.

3. Modeling the random external excitation

The linear filtering technique is widely used in the engineering community for its practicality and simplicity. Dostal and Kreuzer [9] proposed a second-order linear filter and a fourth-order linear filter to fit the desired narrow-banded spectrum. In this work, the spectrum of the relative random external excitation, $S_m(\omega)$, can be approximated by the following second-order linear filter:

$$\begin{cases} dx_3 = (x_4 - \beta x_3)dt + \gamma dW \\ dx_4 = -\alpha x_3 dt \end{cases} \tag{14}$$

where x_3 and x_4 are the state variables in the filter equation with x_3 representing the output term $m(t)$. $dW(t) = W(t+dt) - W(t)$ represents an infinitesimal increment of a standard Wiener process with $E\{dW(t)\} = 0$ and $E\{dW(t)dW(s)\} = 0$ for $t \neq s$ and $E\{dW(t)^2\} = dt$. The spectrum generated by the differential Eq. (14) is given by:

$$S_{2nd}(\omega) = \frac{1}{2\pi} \frac{\gamma^2\omega^2}{(\alpha - \omega^2)^2 + (\beta\omega)^2} \tag{15}$$

in which α, β, γ are the parameters of the linear filter and they are determined by means of a least-square algorithm which is utilized in order to fit of the target spectrum, $S_{mm}(\omega)$. The bandwidth and the peak frequency of the filtered spectrum can be adjusted by changing the values of these parameters.

By combining Eq. (13) with Eq. (15), the extended dynamic system is formed. Therefore, the roll motion in random beam seas with steady mean wind action can be described by the following 4D state space equation:

$$\begin{cases} dx_1 = x_2 dt \\ dx_2 = (-b_{44}x_2 - b_{44q}x_2|x_2| - c_1x_1 + c_3x_1^3 + x_3 + \bar{m}_{wind})dt \\ dx_3 = (x_4 - \beta x_3)dt + \gamma dW \\ dx_4 = -\alpha x_3 dt \end{cases} \tag{16}$$

4. Path integration method

Eq. (16) represents a Markov dynamic system and it can be expressed as an Itô stochastic differential equation (SDE):

$$d\mathbf{x} = \mathbf{a}(\mathbf{x}, t)dt + \mathbf{b}(t)d\mathbf{W}(t) \tag{17}$$

where $\mathbf{x}(t) = (x_1(t), \ldots, x_4(t))^{\mathrm{T}}$ is a 4D state space vector process, the vector $\mathbf{a}(\mathbf{x},t)$ is the drift term and $\mathbf{b}(t)d\mathbf{W}(t)$ represents the diffusive term. The vector $d\mathbf{W}(t) = \mathbf{W}(t+dt) - \mathbf{W}(t)$ denotes independent increments of a standard Wiener process.

The solution $\mathbf{x}(t)$ to Eq. (17) is a Markov process and its transition probability density (TPD), also known as the conditional PDF, $p(\mathbf{x},t|\mathbf{x}',t')$ satisfies the FP equation which is expressed on the following form:

$$\frac{\partial}{\partial t}p(\mathbf{x}, t|\mathbf{x}', t') = -\sum_{i=1}^{4} \frac{\partial}{\partial x_i} a_i(\mathbf{x}, t)p(\mathbf{x}, t|\mathbf{x}', t') + \frac{1}{2}\sum_{i=1}^{4}\sum_{j=1}^{4} \frac{\partial^2}{\partial x_i \partial x_j}(b(t)\cdot b^T(t))_{ij}p(\mathbf{x}, t|\mathbf{x}', t') \tag{18}$$

The PI method captures the probabilistic evolution of the process $\mathbf{x}(t)$ by taking advantage of the Markov property and the PDF of the process $\mathbf{x}(t)$ can be determined by the following basic equation:

$$p(\mathbf{x}, t) = \int_{R^4} p(\mathbf{x}, t|\mathbf{x}', t')p(\mathbf{x}', t')d\mathbf{x}' \tag{19}$$

where $d\mathbf{x}' = \prod_{i=1}^{4} dx_i'$.

Specifically, the value of the PDF at time t, $p(\mathbf{x},t)$, can be calculated by Eq. (19) based on the values of the previous PDF at time t' as well as the value of the conditional PDF, $p(\mathbf{x},t|\mathbf{x}',t')$. For a numerical solution of the SDE (17), a time discretized approximation should be introduced. Naess and Moe [10] proposed an efficient fourth-order Runge–Kutta–Maruyama (RKM) discretization approximation:

$$\mathbf{x}(t) = \mathbf{x}(t') + \mathbf{r}(\mathbf{x}(t'), t')\Delta t + b(t')\Delta\mathbf{W}(t') \tag{20}$$

where the vector $\mathbf{r}(\mathbf{x}(t'), t')$ is the explicit fourth-order Runge–Kutta (RK4) increment. The time sequence $\{\mathbf{x}(i\cdot\Delta t)\}_{i=0}^{\infty}$ is a Markov chain and it can approximate the time-continuous Markov process solution of the SDE (17) when the time increment $\Delta t = t - t'$ is sufficiently small. Since $\mathbf{W}(t)$ is a Wiener process, the independent increment $\Delta\mathbf{W}(t') = \mathbf{W}(t) - \mathbf{W}(t')$ is a Gaussian variable for every t'.

If we consider only the deterministic part of Eq. (10), the approximation Eq. (20) reduces to the RK4 approximation $\mathbf{x}(t) = \mathbf{x}(t') + \mathbf{r}(\mathbf{x}(t'),t')\Delta t$. Experiments have shown that, for the Markov systems, the accuracy related to approximation of the deterministic terms is most important [11]. In this regard, the accuracy of the fourth-order RKM approximation is satisfactory since the fourth-order Runge–Kutta approximation represents the time evaluation of the deterministic part of Eq. (17) with an accuracy to the order of $O(\Delta t^5)$.

Moreover, the conditional PDF of the process $\mathbf{x}(t)$, $p(\mathbf{x},t|\mathbf{x}',t')$, follows a (degenerate) Gaussian distribution and it can be written as:

$$p(\mathbf{x}, t|\mathbf{x}', t') = \delta(x_1 - x'_1 - r_1(\mathbf{x}', \Delta t)) \cdot \delta(x_2 - x'_2 - r_2(\mathbf{x}', \Delta t)) \cdot \tilde{p}(x_3, t|x'_3, t') \cdot \delta(x_4 - x'_4 - r_4(\mathbf{x}', \Delta t)) \tag{21}$$

where $\tilde{p}(x_3, t|x_3', t')$ is given by the relation:

$$\tilde{p}(x_3, t|x_3', t') = \frac{1}{\sqrt{2\pi\gamma^2\Delta t}} \cdot \exp\left\{-\frac{(x_3 - x'_3 - r_3(\mathbf{x}', \Delta t))^2}{2\gamma^2\Delta t}\right\} \tag{22}$$

in which $r_i(\mathbf{x}', \Delta t)$, $i=1, 2, 3, 4$, are the Runge–Kutta increments for the state space variables.

Because the expression for the conditional PDF is known, the time evolution of the PDF of $\mathbf{x}(t)$ can be determined by the iterative algorithm (16) if an initial PDF $p(\mathbf{x}^{(0)}, t_0)$ is given

$$p(\mathbf{x}, t) = \int_{R^4} \cdots \int_{R^4} \prod_{i=1}^{n} p(\mathbf{x}^{(i)}, t_i|\mathbf{x}^{(i-1)}, t_{i-1}) \cdot p(\mathbf{x}^{(0)}, t_0) d\mathbf{x}^{(0)} \ldots d\mathbf{x}^{(n-1)} \tag{23}$$

where $\mathbf{x} = \mathbf{x}^{(n)}$, $t = t_n = t_0 + n \cdot \Delta t$.

As for the numerical implementation of the iterative algorithm (23), it represents the PDF at the previous time t' as an interpolating spline surface via Parabolic B-spline and then it evaluates the PDF at time t by several specific steps. The initial PDF $p(\mathbf{x}^{(0)}, t_0)$ is chosen as a 4D Gaussian PDF with zero mean and variances evaluated by a simple Monte Carlo simulation [11]. The numerical iterative algorithm and the associated specific computational steps have been systematically described by Chai et al. [4].

5. Numerical results

5.1. Random external excitation

In this section, the importance of the random external excitation, i.e., $m_{wave}(t)$ and $m_f(t)$ in Eq. (11) is studied. A real ship model in Ref. [12] is selected for the simulation. The main parameters of the vessel are shown in Table 1 and *GZ* curve for the selected ship model is plotted in Fig. 1.

The modified Pierson–Moskowitz (P–M) spectrum, widely used for fully developed sea states, is adopted in this analysis.

$$S_{\xi\xi}(\omega) = \frac{5.058 g^2 H_s^2}{T_p^4 \omega^5} \exp\left(-1.25 \frac{\omega_p^4}{\omega^4}\right) \tag{24}$$

in which H_s denotes the significant wave height, ω_p is the peak frequency at which the wave spectrum $S_{\xi\xi}(\omega)$ has its maximum, and T_p is the corresponding peak period.

Table 1
List of parameters for the vessel.

Parameters	Dimensional value
$I_{44} + A_{44}$	5.540×10^7 kg m^2
Δ	2.017×10^7 N
A_w	620 m^2
l_w	6.85 m
b_{44}	0.095 s^{-1}
b_{44q}	0.0519
c_1	1.153 s^{-2}
c_3	0.915 s^{-2}
ω_0	1.074 rad/s

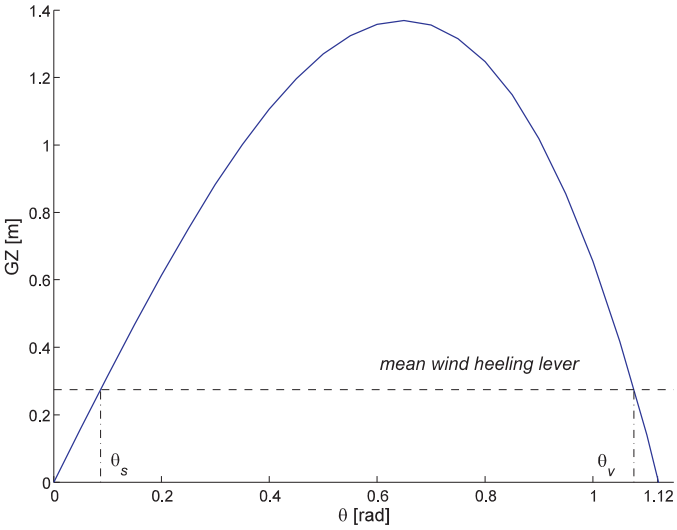

Fig. 1. *GZ* curve for the selected vessel.

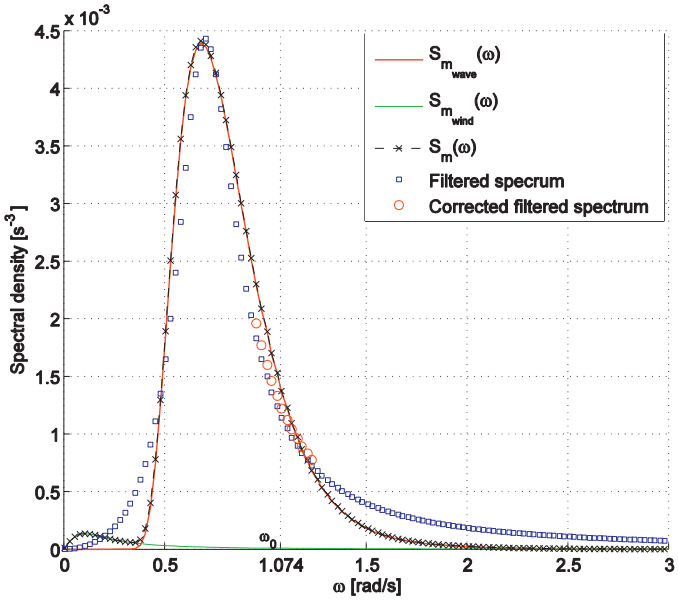

Fig. 2. Relative wave excitation moment spectrum, relative fluctuating wind spectrum, relative spectrum of total relative random external excitation, filtered spectrum and the corrected filtered spectrum (part).

The sea state with $H_s = 4.0$ m, $T_p = 11.0$ s is selected for the subsequent study and the wave excitation spectrum $S_{Mwave}(\omega)$ is then determined by Eq. (3) with the relevant information of $|F_{roll}(\omega)|$ being given in Ref. [12]. For the spectrum of the fluctuating wind moment, the mean wind speed U_m is selected as 26 m/s according to weather criterion of the IMO and the wind pressure coefficient $C_w = 0.95$ [13].

The spectrum of the relative wave excitation moment, $S_{m_{wave}}(\omega)$ for the selected sea state, the spectrum of the relative fluctuating wind moment $S_{m_f}(\omega)$ for the selected mean wind speed and the corresponding spectrum of total relative random external excitation, $S_m(\omega)$ are shown in Fig. 2. For the roll motion, the transfer function between the roll excitation moment and the roll response in the SDOF model (1)

is narrow-banded due to the light roll damping. Therefore, the value of $S_m(\omega)$ in the critical region near the natural roll frequency, ω_0, dominates the subsequent roll response. It can be seen in Fig. 2 that $S_{m_f}(\omega)$ is peaked in the low-frequency region and its value in the critical region is negligible when compared with the values of $S_{m_{wave}}(\omega)$ and $S_m(\omega)$. Therefore, the influence of fluctuating wind moment on the stochastic roll response can be neglected in the simulation.

As mentioned in Section 3, the relative random external excitation, $S_m(\omega)$, can be approximated by a second-order linear filter, whose parameters are determined by means of a least-square algorithm. The fitting result is shown in Fig. 2 that the filtered spectrum is reasonable in terms of bandwidth, peak frequency and peak value. The obvious discrepancies between the filtered spectrum and the desired spectrum in the low-frequency and high-frequency regions will not influence the subsequent roll responses to a significant extent. However, in the critical region near the natural roll frequency, the slight discrepancy between the two spectra should not be neglected since the distribution of high-level response is sensitive to the variation of the external excitation in this frequency region.

Therefore, a constant, c, should be introduced as a correction factor for the filtered spectrum in order to reduce the discrepancy in the critical frequency region. The filtered spectrum (15) can be changed into:

$$S_{2nd}(\omega) = \frac{1}{2\pi}\frac{(c\cdot\gamma)^2\omega^2}{(\alpha-\omega^2)^2+(\beta\omega)^2} \tag{25}$$

In this work, for the selected sea state and vessel model, the correction factor c is taken to be 1.07 by considering the mean difference between the two spectral densities in the critical frequency region. Moreover, the corrected filtered spectrum in the critical frequency region is also presented in Fig. 2.

Even though the influence of fluctuating wind moment m_f on the stochastic roll response can be neglected for the selected vessel, the effect of the mean wind action on the response statistics and ship stability is important and it will be studied in the following section.

5.2. Reliability evaluation

The reliability evaluation is usually phrased in terms of the probability of a stochastic process exceeding a threshold level ζ at least once within time duration T [14]. In this paper, the second category of the intact stability failure, i.e. the reliability associated with high level response, is considered. The Poisson estimate is available if the crossing events are assumed to be rare and statistically independent. Under such an assumption, the crossing events are Poisson distributed and the probability that the roll angle process exceeds the threshold level ζ at least once within time duration T, $P_{exc}(\zeta)$, can be approximated as:

$$P_{exc}(\zeta) = 1-\exp\left(-\int_0^T \nu^+(\zeta;t)dt\right) \tag{26}$$

where $\nu^+(\zeta;t)$ denotes the expected number of upcrossings for the ζ-level per unit time at time t by the roll angle process $\theta(t)$. By taking advantage of the joint PDF of the roll angle process and the roll velocity process obtained by the 4D PI technique, the mean upcrossing rate can be given by the Rice formula:

$$\nu^+(\zeta;t) = \int_0^\infty \dot\theta f_{\theta\dot\theta}(\zeta,\dot\theta;t)d\dot\theta \tag{27}$$

in which $f_{\theta\dot\theta}(\theta,\dot\theta;t)$ is the joint PDF of the roll angle and the roll velocity at the time instant t.

As mentioned in Section 2, due to the softening characteristic of the stiffness term, ship capsizing will happen when the predetermined simulation time (or exposure time) T is long enough or the intensity of the external excitation is strong enough. If the mean time to capsize is long enough, the dynamic system can be regarded as a highly reliable system and the corresponding roll response reaches stationary in an approximate sense [6]. Therefore, the practical time-variant upcrossing rate $\nu^+(\zeta;t)$ can be approximated as a time-invariant parameter $\nu^+(\zeta)$ at a suitable reference point in time.

The straightforward Monte Carlo simulation can serve as a validation for the upcrossing rate obtained by the 4D PI method and the Rice formula (26). For a stationary sea state, the appropriate sample mean value of the upcrossing rate can be obtained from the time histories of the roll angle process:

$$\hat\nu^+(\zeta) = \frac{\sum_{i=1}^k n_i^+(\zeta;T_i)}{\sum_{i=1}^k T_i} \tag{28}$$

Where $n_i^+(\zeta;T_i)$ denotes the counted number of upcrossings for the level ζ within a time duration of length T_i for simulated time history no. i. The practical simulation time T_i is not fixed for each simulation, but it is equal to the predetermined simulation time T if no capsizing occurs. Otherwise, it is the value of termination time t_i for each case where capsizing occurs. Moreover, the number of simulations, k, e.g. $k=1000$–5000, is selected according to the values of upcrossing rates in the tail region and the length of the predetermined simulation time T. Usually, low upcrossing rates and short time periods T correspond to a large simulation number k.

A fair approximation of the 95% confidence interval, $CI_{0.95}$, can be expressed as [15]:

$$CI_{0.95}(\zeta) = \left(\hat\nu^+(\zeta)-1.96\frac{\hat s(\zeta)}{\sqrt{k}}, \hat\nu^+(\zeta)+1.96\frac{\hat s(\zeta)}{\sqrt{k}}\right) \tag{29}$$

where the empirical standard deviation $\hat s(\xi)$ is given as:

$$\hat s(\zeta)^2 = \frac{1}{k-1}\sum_{i=1}^k\left(\frac{n_i^+(\zeta;T_i)}{T_i}-\hat\nu^+(\zeta)\right)^2 \tag{30}$$

For the selected sea state, the upcrossing rate calculated by application of the 4D PI method and the empirical estimation of the upcrossing rate $\nu^+(\zeta)$ as well as the 95% confidence interval obtained by Monte Carlo simulation are shown in Fig. 3. In the Monte Carlo simulation, long time domain simulations are needed to obtain upcrossing rates for high response levels. For this case, the simulation number k

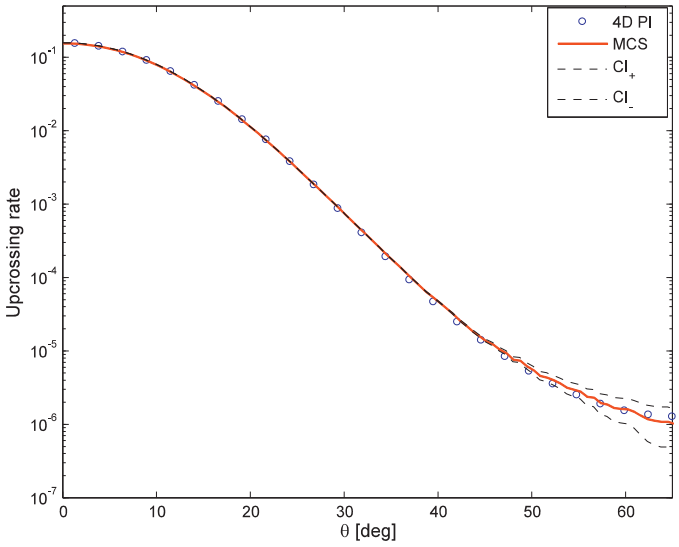

Fig. 3. Upcrossing rates for the vessel without initial heeling obtained by the 4D PI method and Monte Carlo simulation (MCS) for the sea state with $H_s = 4.0$ m, and $T_p = 11.0$ s.

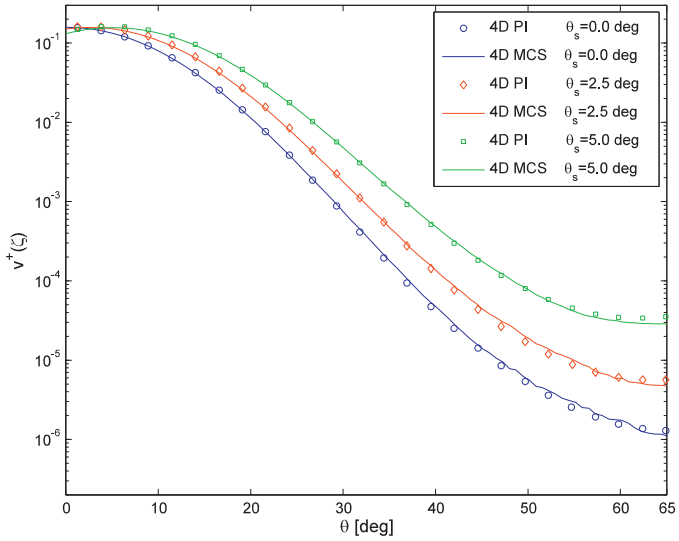

Fig. 4. Influence of the heeling angle on the upcrossing rate, for the sea state with $H_s = 4.0$ m, and $T_p = 11.0$ s.

is selected to be 3000 and the predetermined simulation time T is 1.0×10^5 s.

The mean wind action results in an initial (or permanent) heeling angle θ_s and the corresponding mean wind heeling level is shown in Fig. 1. Fig. 4 presents its influence on the upcrossing rate. It can be readily seen that the existence of heeling angle increases the upcrossing rate, which indicates that the vessel with heeling angle would cross the high response levels more frequently than the vessel in the upright condition. Moreover, Figs. 3 and 4 demonstrate that the 4D PI technique yields accurate and reliable calculation of the upcrossing rates, even in the high roll response region.

For high response levels, let $\Theta(t) = \max\{\theta(t):0 \le t \le T\}$ denote the largest value of the roll angle process $\theta(t)$ over the time interval of length T [2]. If the random number of upcrossing in an arbitrary time interval of length T is Poisson distributed, the cumulative distribution function (CDF) of the extreme value $\Theta(t)$ for the exposure period T can be given in terms of the mean upcrossing rate by the following relation for a stationary short-term sea state:

$$F_{\Theta(T)}(\zeta) = \exp\left(-\int_0^T v^+(\zeta;t)dt\right) \approx \exp\left\{-v^+(\zeta)\cdot T\right\} \tag{31}$$

Moreover, the empirical estimation of the exceedance probability obtained by Monte Carlo simulation is given as:

$$P_{MC}(\zeta, T) = 1 - F_{MC}(\zeta, T) \tag{32}$$

where $F_{MC}(\xi,T)$ is the empirical CDF of the extreme value $\Theta(t)$ over the time interval of length T, which can be evaluated in terms of simulated maximum roll angles ranked in ascending order. Furthermore, for Monte Carlo simulation, the exceedance probability for the high-level responses converges toward a normal distribution for a large number of realizations, N_t and the 95% CI of the exceedance probability during the exposure time T can be given as:

$$CI_{0.95}(P_{MC}) = \left(P_{MC} - 1.96\sqrt{\frac{P_{MC}\cdot(1-P_{MC})}{N_t}}, P_{MC} + 1.96\sqrt{\frac{P_{MC}\cdot(1-P_{MC})}{N_t}}\right) \tag{33}$$

Correspondingly, the influence of the initial heeling angle on the CDF is shown in Fig. 5 and Figs. 6–8 present the

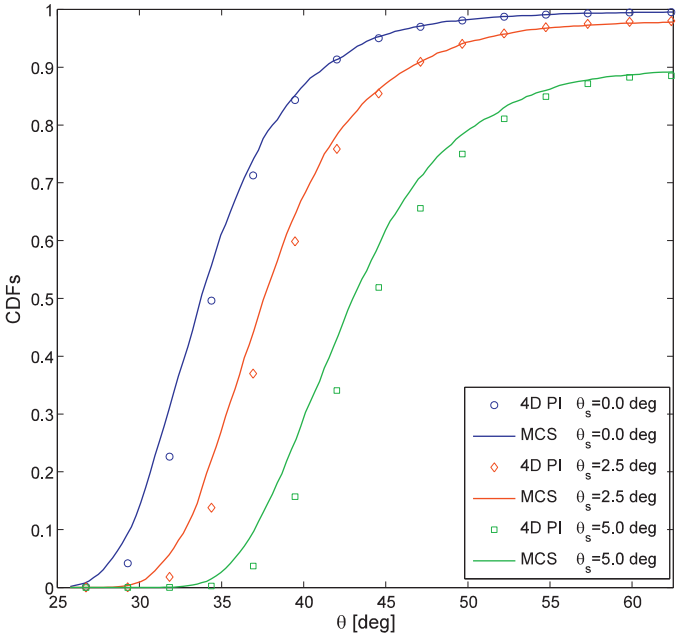

Fig. 5. Influence of the heeling angle on the distribution of high level responses for the sea state with $H_s = 4.0$ m, $T_p = 11.0$ s, and exposure time $T = 1$ h.

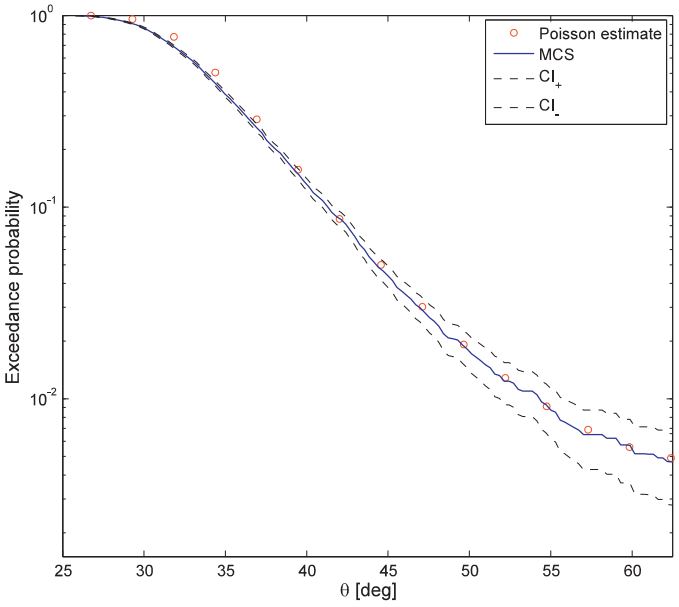

Fig. 6. Exceedance probability of high level responses for the vessel without initial heeling, exposure time $T=1$ h.

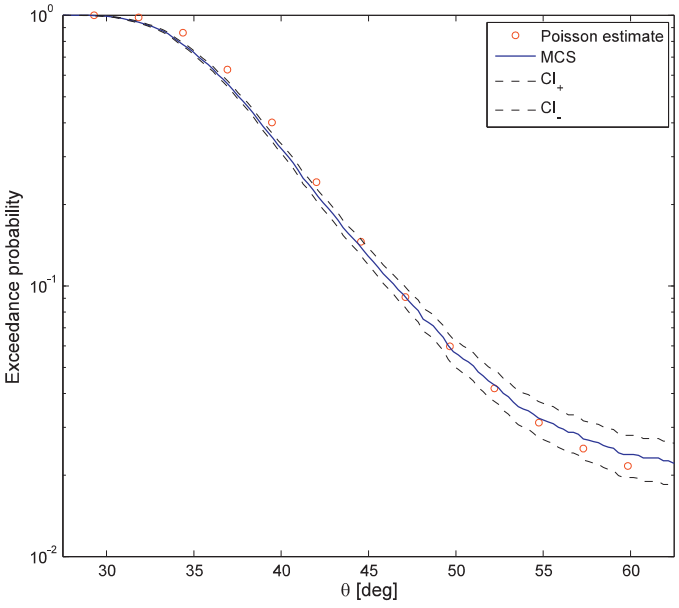

Fig. 7. Exceedance probability of high level responses for the vessel with 2.5° initial heeling angle, exposure time $T=1$ h.

effect of the initial heeling angle on the exceedance probability of high level response. The empirical CDFs and empirical exceedance probabilities as well as the confidence intervals obtained by the Monte Carlo simulation results are also plotted in these figures in order to verify the results obtained by Eqs. (31) and (32). The number of realizations, N_t, for each case is selected to be 5000 and the reference exposure period, T is 1 h for each realization [1].

The comparisons in Figs. 5–8 demonstrate a quantitative measure of the common sense that the heeling angle deteriorates the vessel's stability. A small heeling angle obviously

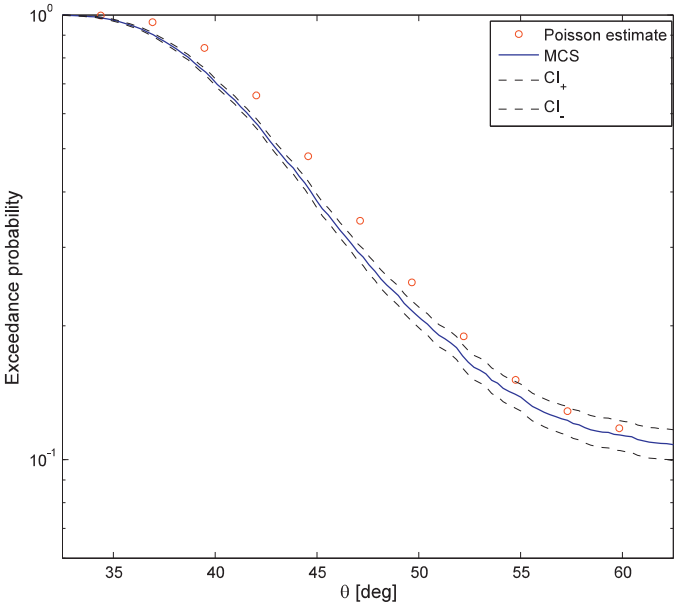

Fig. 8. Exceedance probability of high level responses for the vessel with 5.0° initial heeling angle, exposure time $T=1$ h.

influence the reliability of the vessel illustrates that ship stability in random beam seas is sensitive to the existence of the heeling angle. In addition, it is seen in Fig. 5 that the accuracy of the Poisson estimate is satisfactory on the whole, but the accuracy declines as the roll response increases. This tendency can also be observed in Figs. 6–8, e.g. the Poisson assumption provide excellent estimations for the case without heeling angle and for the case with 2.5° heeling angle. However, in Fig. 8, when the heeling angle increases to 5°, the Poisson estimate slightly overestimates the exceedance probabilities of a part of the high-response levels.

Generally, the simple Poisson assumption is widely used to predict the failure probability of structures subjected to random excitations. For a large ship, the exceedance probability of a high-response level is important since a number of other damages will occur at large angles. However, when the response increases, the accuracy of the Poisson estimate gradually declines because the assumption of Poisson distributed upcrossing tend to be less invalid [4]. On the other hand, the Poisson estimate can take advantage of the reliable response statistics obtained by the 4D PI method. Its simplicity and accuracy, as presented in Figs. 5– 8, is attractive for practical applications to evaluate the exceedance probabilities of large or extreme roll angles, but except for very serious response. For the selected mean wind speed $U_m=26$ m/s, it results in a permanent heeling angle θ_s=1.54° and the Poisson assumption can provide satisfactory estimations.

6. Conclusions

In this work, the 4D PI method, based on the Markov property of the dynamic system, was introduced to analyze the stochastic roll response and the reliability for a vessel rolling in random beam seas and beam wind. Based on the

results and discussions mentioned above, several conclusions can be drawn as follows.

For the selected vessel model, the influence of the fluctuating wind moment on the stochastic roll response can be neglected because the spectrum of the fluctuating wind moment is peaked in the low-frequency region, which is far away from the critical frequency region near the natural roll frequency. But for the vessels with very large natural roll periods (e.g. 30 s), the effect of fluctuating wind action could be a possible critical problem.

The mean wind action significantly influences the stochastic roll response and deteriorates the ship stability in random waves. The good agreements of the results obtained by the proposed numerical results and the Monte Carlo simulation results demonstrate the reliability of the 4D PI method as well as the rationality of the Poisson distributed approximation.

Furthermore, the permanent heeling moment can also be caused by transverse displacements of masses or by the lateral pull in the towing work, etc. [16]. Therefore, current study with respect to the influence of the mean wind action as well as the method used in this study is also applicable for other cases with initial heeling moments.

Acknowledgments

This work is supported by China Scholarship Council (CSC) (Grant no. 201306230077), affiliated with the Ministry of Education of the P.R. China. The suggestions from Prof. Arvid Naess and Prof. Bernt J. Leira are gratefully acknowledgement.

References

[1] ITTC (2011), Stability in Waves Committee – Final report and recommendations to the 27th ITTC, in: Proceedings of the 27th International Towing Tank Conference.
[2] A. Naess, T. Moan, Stochastic Dynamics of Marine Structures, Cambridge University Press, United Kingdom, 2012.
[3] W. Chai, A. Naess, B.J. Leira, Probab. Eng. Mech. (2016) (in press), doi:10.1016/j.probengmech.2015.10.002.
[4] W. Chai, A. Naess, B.J. Leira, J. Ship Res. 59 (2015) 113–131 http://dx.doi.org/10.5957/JOSR.59.2.140059 .
[5] W. Chai, A. Naess, B.J. Leira, Probab. Eng. Mech. 41 (2015) 104–114, doi:10.1016/j.probengmech.2015.06.002.
[6] J. Roberts, M. Vasta, Philos. Trans. R. Soc. Lond. Ser. A: Math. Phys. Eng. Sci. 358 (2000) 1917–1941, doi:10.1098/rsta.2000.0621.
[7] M. Gu, J. Lu, T. Wang, J. Hydrol., 27(2015), 452–457, doi:10.1016/S1001-6058(15)60503-0.
[8] G. Bulian, A. Francescutto, Proc. Inst. Mech. Eng. Part M: J. Eng. Marit. Environ. 218 (2004) 189–212, doi:10.1243/1475090041737958.
[9] L. Dostal, E. Kreuzer, Proc. Inst. Mech. Eng. Part C: J. Mech. Eng. Sci. 225 (2011) 2464–2476, doi:10.1177/0954406211414523.
[10] A. Naess, V. Moe, Probab. Eng. Mech. 15 (2000) 221–231, doi:10.1016/S0266-8920(99)00031-4.
[11] E. Mo, Nonlinear stochastic dynamics and chaos by numerical path integration (Ph.D. thesis), Norwegian University of Science and Technology, Trondheim, Norway, 2008.
[12] Z. Su, Nonlinear response and stability analysis of vessel rolling motion in random waves using stochastic dynamical systems (Ph.D. thesis), Texas A&M University, Texas, USA, 2012.
[13] I.M.V. Andersen, Ocean Eng. 58 (2013) 115–134, doi:10.1016/j.oceaneng.2012.10.008.
[14] Y. Low, Probab Eng Mech 24 (4) (2009) 565–576, doi:10.1016/j.probengmech.2009.04.002.
[15] A. Naess, O. Gaidai, P. Teigen, Appl. Ocean Res. 29 (2007) 221–230, doi:10.1016/j.apor.2007.12.001.
[16] A. Biran, R.L. Pulido, Ship Hydrostatics and Stability, Butterworth-Heinemann, United Kingdom, 2013.